Automated Data Reduction at a Small College Observatory

Donald A. Smith
Physics Department, Guilford College, 5800 W. Friendly Avenue, Greensboro, NC 27410; dsmith4@guilford.edu

Hollis B. Akins
Physics Department, Grinnell College, 1116 Eighth Avenue, Grinnell, IA 50112

Received July 15, 2019; revised August 14, 2019; accepted August 30, 2019

Abstract We report on our success in automating the data analysis processes for a small (half-meter class) reflecting telescope at Guilford College, a small liberal arts college in an urban location. We give a detailed description of the hardware that makes up the instrument. We use commercial software to run the telescope, and we have written Python scripts to automatically carry out the daily tasks of image reduction, source extraction, and photometric calibration of the instrumental magnitudes to the AAVSO APASS catalogue. We characterize the effect of light pollution in terms of sky brightness and typical limiting magnitudes ($V \sim 15$ for a 60-s image), and we report that our RMS scatter in light curves for constant sources approaches 0.5% for bright ($V < 10$) sources. As a test of our system, we monitored two known variable stars, and we confirm the predicted ephemerides as given by the AAVSO web site target tool. We hope that this paper will provide a context in which future observations reported from this site can be interpreted.

1. Introduction

The Guilford College Cline Observatory is a primarily educational resource for students interested in learning about observational astronomy. An array of small reflecting telescopes can be set up on clear nights to allow beginners, photographers, and the public to view the night sky. With solar filters and an Hα scope, we enable the observations of sunspots and eclipses. Two 2.4-m radio telescopes extend our vision to the 21-cm neutral hydrogen line. In recent years, however, we have endeavored to bring the primary optical telescope into a reliably automated state such that it can more robustly contribute to scientific research.

In this paper, we report on the technical specifications of the 16-inch optical telescope and our automated data processing pipeline. We detail the structure and characterize the performance of the pipeline; every morning it reduces the images recorded by the telescope the previous night. This software also extracts a list of sources from every image and calibrates their instrumental magnitudes to the AAVSO APASS catalogue.

The result is an ever-updating database of brightness measurements that can be used to construct light curves, perform brightness distribution studies, and monitor stars that have been flagged as of interest by the AAVSO. We intend this paper to characterize the specifics of our instrument so that future reports and updates from our site can be understood. In a separate paper, we plan to report on our efforts to set up an accompanying spectroscopic telescope that can be used in conjunction, simultaneously, with the automated photometric telescope. This will be useful, as both telescopes will share the same observing conditions.

In section 2, we lay out the technical specifications of the hardware and software that make up the telescope. We follow, in section 3, with a short description of the observing conditions that our urban environment affords us. Section 4 describes the design and operation of the data reduction and analysis pipeline, and section 5 presents two examples of the results our observatory can provide. We close with a short description of what we hope to offer in future work. It is our hope that this paper will provide the reader the context to evaluate the strengths and challenges underlying future science reports.

2. Telescope components and control

The centerpiece of the observatory is a 6-m diameter Observadome. The dome opens a 1.6-m wide slit using two laterally sliding gate doors. Power is conveyed to the dome from below using seven circular rails with sliding conductive contacts, enabling unrestricted rotation in either direction. The hemispherical dome rests on eight spring-loaded tires, and rotation is driven by two friction-drive wheels. An optical sensor counts wheel rotations and allows the calculation of angular displacement. A magnetic switch defines the home position. A wall-mounted enclosure contains the two circuitboards of a MAXDOME II automation system (Diffraction Limited 2019a) and four relays wired in parallel with the manual buttons. We have also installed wireless communication between the MAXDOME boards and the slit window motors, as the unrestricted rotation of the dome disallows any attempt to run a wire across the boundary. This system enables computer control of dome rotation and slit operation. The dome also has a wind shield that can move up and down, but we have not automated this feature and generally leave the shield down.

At the center of the dome is a 16-inch RCOS reflecting telescope (f/8.3). The focal length of 3.4 m yields an image scale of 61 arcsec/mm at the focal plane. This closed truss optical tube is mounted on a Paramount ME robotic telescope mount (Software Bisque 2019a). The entire instrument rests on a sand-filled pier, 30 cm in diameter. This pier sits on a steel I-beam, which extends 70 cm to the North (center to center) from a 80-cm diameter cylindrical concrete base. The base is acoustically isolated from the metal floor, and rests on a skeletal structure that is isolated from the rest of the building. The result is that the rotation axes of the telescope cross roughly three meters

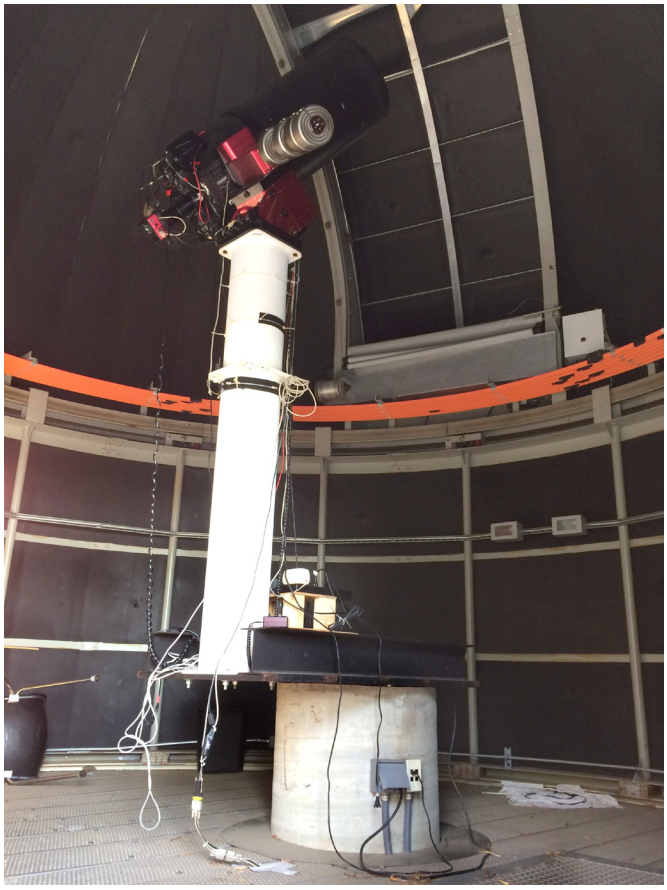

Figure 1. Image of the inside of the dome. The cantilevered pier is visible at the bottom of the image—the concrete acoustically isolated base, the black I-beam, and the white sand-filled pier. The Paramount ME and the RCOS telescope are on top, with the CCD camera to the left. The dome slit is visible in the background. The orange curves are the rails that carry AC power to the dome from below.

above the floor, to put the telescope at the geometric center of the dome. Figure 1 shows the interior of the dome, from the concrete base up to the RCOS OTA.

The cantilevered offset of the pier was the result of a compromise between scientific functionality and the aesthetics of how the dome would look from a distance. Although we worried that the cantilever structure might introduce harmful vibrations into the observing process, an undergraduate thesis project revealed that in the absence of humans, neither the dome's rotation nor the mount's slewing introduced any measurable jitter into the images (Corbett 2011). The same research found that vibrations created by striking the pier directly faded with an e-folding time of less than 30-s. Automated operations have never revealed significant degradation due to pier oscillations.

Images are captured with an SBIG STF-8300M CCD camera (Diffraction Limited 2019b). This instrument has 3326 × 2504 pixels at 5.4 microns, yielding an image scale of 0.33 arcsec/pix at the chip. The shutter is designed to afford even illumination over the entire chip, and the full-frame readout time is less than one second. The camera is outfitted with an FW8 filter wheel. We have chosen to use Baader Red, Green, and Blue filters for astrophotography, and Bessel R, V, and B filters for photometry. The final two slots contain an Hα filter and an open, "Lum" filter. Focus is driven by a motor that moves the secondary mirror along the optical axis. This motor is controlled by the RC Optical Systems Telescope Command Center (TCC-I; Deep Sky Instr. 2019). The STF-8300 has the capability to add a secondary camera for autoguiding, but we have not yet implemented this feature.

We have two devices to monitor the weather. An Aurora Cloud Sensor (Aurora Eurotech 2019) measures the difference between the sky temperature and the ambient air temperature to estimate cloud cover, and an exposed sensor reports the presence of rain drops. A Davis Vantage Vue weather station (Davis Instr. 2019) records humidity, pressure, wind speed and direction, and temperature. These data are recorded and stored on the central computer.

All the features of this telescope system are controlled via computer. As of May 2019, the control computer is a Hewlett-Packard HPE-470F Pavillion Elite, running 64-bit Windows 10. Software Bisque's THESKYX (2019b) anchors the system, connecting to the mount, focuser, camera, and dome. Aurora and Davis provide their own software to connect to the weather stations. We have augmented THESKYX with the TPoint and All Sky ImageLink features. The mount, camera, and focuser are plugged into a IP-enabled power strip so that sockets may be turned on and off individually through a web browser interface, and we have a wall-mounted IR-enabled Foscam security camera. These features allow us to operate the facility remotely using the TeamViewer program as a remote desktop. The use of TeamViewer's App makes it possible to run the whole operation from the screen of a mobile phone.

THESKYX can receive scripted commands over the Internet. We have written programs to schedule a night's observations without human intervention. The python programs are stored on a Linux computer in another room in the building. Each script starts with targets as a list of strings with associated R.A.and Dec. coordinates (J2000.0). Exposure time, filter choice, and delays between observations are also specified. The script updates the coordinates to the current day's epoch and instructs THESKYX to slew the telescope, wait a desired time to allow the dome and the telescope to both reach the target, and then take an image. Each image is automatically passed to THESKYX's All Sky Image Link process for source identification and the derivation of world coordinate system (WCS) astrometric parameters. This ensures that our images can be seamlessly passed to the analysis pipeline (section 4).

The script includes definitions for procedures to turn all the pieces of the telescope system on at the start of the night as well as code to shut everything down at a pre-determined time. After startup is complete, the script will loop through the indicated observations until the shutdown time is reached. However, we have not yet scripted a connection to the weather monitor, so the system is not yet capable of shutting itself down in the case of unanticipated weather developments. We plan to implement this feature in the future.

3. Urban sky brightness

The Guilford College Cline Observatory (Lat. +36° 5' 42", Lon. –79° 53' 24", altitude 280 m) is situated on the roof of a three-story building that houses the natural sciences offices,

labs, and classrooms. Although the College has committed to replacing outdoor light fixtures with downward facing baffles, and the campus contains more than 100 acres of undeveloped forest, we are still in an urban environment. As of 2019, Greensboro proper houses more than 250,000 inhabitants, and is one of three major cities in an urban area called "The Triad" (also including High Point and Winston-Salem). The center of Greensboro is ~9 km southeast of our location, and the Piedmont Triad International airport is ~ 3 km to the west.

Although the northern skies are slightly darker than the southern, this cannot be considered a dark sky site. A 2001 global light pollution map, based on satellite observations, atmospheric modeling, and other statistics, predicts a range in sky background brightness values from 17.80 to 18.95 magnitudes per square arcsecond of subtended area at Guilford College's location (Cinzano *et al.* 2001). A 2016 student senior thesis project recorded roughly 100 images of two fields with 10 s and 30 s of exposure in each of the Baader Green and Blue filters and found that the actual sky brightness at our location was consistent with approximately 17 mag per sq. arcsec (Seitz 2016).

A follow-up senior thesis project attempted to measure the contribution to sky brightness due to the addition of lights to our primary football field, roughly 500 m southeast of the science building. Turning the field lights on and off had to be coordinated with a company in Iowa, but Oulette (2016) observed multiple fields at an elevation of approximately 30° above the stadium and found that the presence or absence of the field's lights had no significant impact on the sky brightness or limiting magnitude of the images.

Our own observations of open cluster NGC~6811 indicate that for a 60-s exposure, we can expect to reach roughly 15th magnitude. Figure 2 shows a histogram of the number of sources extracted from the field with our automated pipeline. For a 60-s image, there is a steep decline in the number of sources at $V \sim 15$, and no sources at all below $V \sim 15.5$.

Another way to characterize the stability of the analysis is to measure magnitude fluctuations over time. Tracking M29 for the night of 14 July 2019 yielded 35 measurements of 101 stars. The pipeline analysis reported median values of the FWHM for each image that ranged between 1 and 2 arcseconds. Figure 3 shows a plot of the RMS variability in the resulting light curves as a function of the mean magnitude. For stars brighter than $V \sim 11$, the variation is consistent with fluctuations at the ~ 0.005-mag level. Below this brightness, the stability decays, rising to a maximum of 0.07 mag. The statistical uncertainty of the dimmest stars in these 60-s images is ± 0.03 mag.

These fluctuations can be considered an estimate of the systematic uncertainty in the magnitude, and for dim stars they dominate over the statistical error associated with the photon counts. In the next section, we describe the pipeline that produced these measurements.

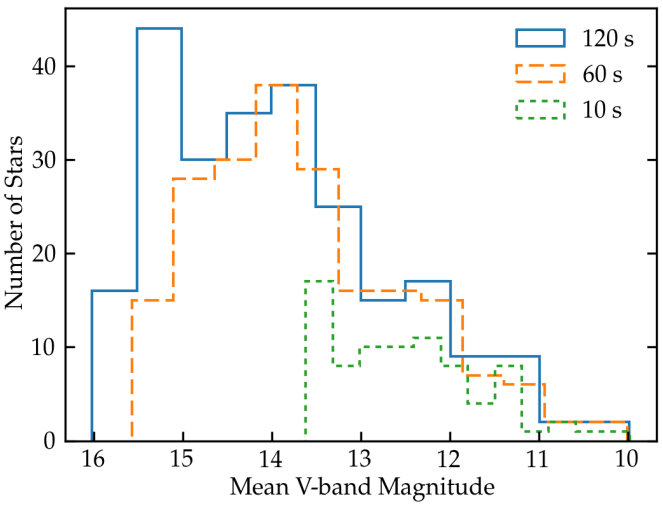

Figure 2. Histogram of number of sources as a function of V-band magnitude for a 10-s exposure (81 stars in green/dotted), a 60-s exposure (203 stars in orange/dashed), and a 120-s exposure (241 stars in blue/solid) of open cluster NGC 6811. The limiting magnitudes can be estimated by seeing where the histogram drops off: V~13.5, 15.0, and 15.5, respectively.

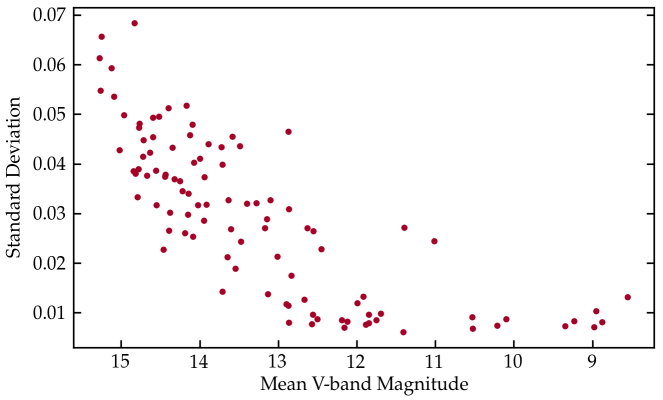

Figure 3. Standard deviation of source brightness as a function of mean magnitude. This graph is derived from 35 observations of 101 sources in open cluster M29 over the course of the night of 14 July 2019. Each image was exposed for 60 s. Fluctuation levels approach 0.5% for sources brighter than $V \sim 11$, but degrade to 0.07 mag at a magnitude of $V \sim 15.5$. These RMS values can be interpreted as an estimate of the systematic uncertainty in our ensemble photometry method.

4. Data analysis pipeline

We have developed software to reduce and analyze all images captured with the 16-inch telescope, based on the pipeline used in the ROTSE-III telescope system (Akerlof *et al.* 2003; Smith *et al.* 2003). The pipeline consists of python scripts housed on a Linux computer. The data directories on the telescope control computer are remote-mounted on the Linux computer for easy access. All images are recorded in the FITS format (Wells *et al.* 1981).

The primary script is launched via a cron utility every morning. If the script ascertains that new images have been recorded in the last night, it copies them to the Linux computer. It then applies dark, bias, and flat-field corrections to create a new archive of calibrated images, using the ASTROPY package (Astropy Collaboration *et al.* 2013). The script also checks to see if new calibration files have been recorded. If possible, new calibration masters are made from individual files to ensure up-to-date correction images.

Any further pipeline processing requires the image to have WCS conversion equations recorded in the FITS headers. If the images were not solved at the time they were recorded

Table 1. Observing targets.

Star	*R.A. (J2000)* *h m s*	*Dec. (J2000)* *° ′ ″*	*Date*	*Type*	*T*[a] *(days)*	*Number of Images*	*Cadence (seconds)*	*(N)*[b]
RR Lyr	19 25 27.9	+42 47 03.7	2018-08-15	RR	0.57	73	160	86
V457 Lac	22 36 23.0	+38 06 18.4	2018-08-16	E	6.16	29	800	101

[a] *From The AAVSO International Variable Star Index (VSX; Watson* et al. *2006-2014).* [b] *Average number of sources in field.*

with the ImageLink process within THESKYX (as programmed in our observing PYTHON scripts), a plate solution using nova.astrometry.net, or equivalent, is also sufficient.

Following calibration, in the presence of astrometric data, we use the SExtractor PYTHON wrapper (Barbary 2016) to perform source extraction, annulus subtraction, and aperture photometry. We use a fixed aperture radius of 12 pixels (scaled down linearly at higher pixel binning) and a surrounding annulus with inner and outer radii set to 1.5 to 2.0 times the aperture radius, respectively. Sources with pixel values less than four times the background RMS are discarded. We use an outlier-removal algorithm to account for source contamination, and all stars flagged as saturated or truncated by an image boundary are ignored. This aperture photometry method yields uncalibrated instrumental magnitudes for every source identified in the image.

Next, measured celestial locations of all unsaturated sources are then matched to entries in the AAVSO APASS catalogue (Henden *et al.* 2015), with a tolerance of 3 arcseconds, to retrieve catalogue magnitudes. The median offset between instrumental and catalogue magnitudes is used to correct all the instrumental magnitudes and thereby derive calibrated magnitudes for all sources in the field. This approach is called ensemble photometry (Honeycutt 1992; Everett and Howell 2001). The resulting calibrated magnitudes are saved to a master database along with other identifying information for each source. From this database we can extract light curves.

5. Example results

To test the reliability of the pipeline reduction and analysis process, we chose two variable stars to monitor throughout a night. We used the AAVSO Target Tool (AAVSO 2017) to identify two sources that were predicted to engage in interesting behavior on the nights we would be observing. RR Lyrae, the eponym for the RR Lyrae class of variable stars, was predicted to reach a maximum at approximately 06:30 UT on the morning of 16 Aug 2018, so we expected to see the brightness begin to rise approximately 90 minutes before then. The next night, we monitored V457 Lac, an eclipsing binary that was predicted to have an eclipse event at 03:00 UT.

Table 1 presents details of our two observing programs. It gives the target coordinates and the dates of the observations, the type of the target star, and the period of its variation. The number of images taken each night and the typical time between images are also reported. Both fields held close to 100 sources (last column), more than enough for the ensemble photometry technique, and we obtained over 25 images of each field. We used a Bessel V-band filter for all images.

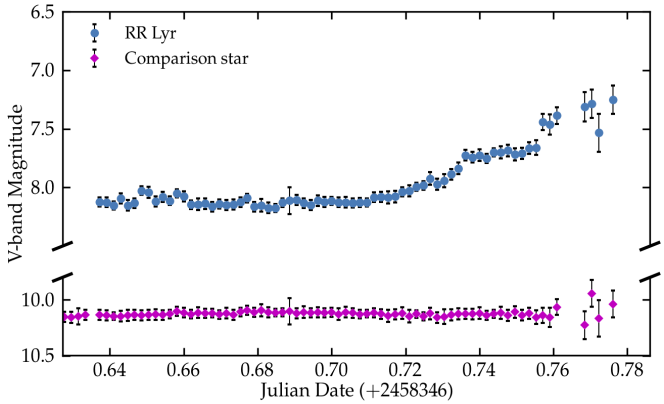

Figure 4. Light curve for RR Lyr from 15 Aug 2018. The light curve for a (constant intensity) comparison star at tenth magnitude is also included to indicate the level of systematic fluctuations in the analysis. Error bars indicate formal statistical uncertainty derived from random counting. The gaps and increased uncertainty towards the end of the observing run are the result of incoming clouds.

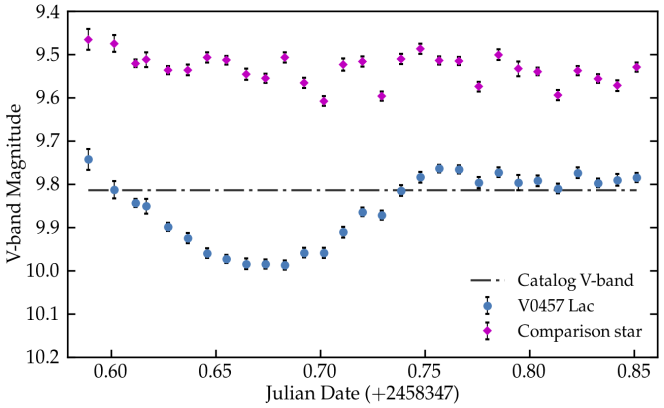

Figure 5. Light curve for V457 Lac, an eclipsing binary, recorded over six hours on the night of 17 Aug 2018. The light curve for a (constant intensity) comparison star is also included to indicate the level of systematic fluctuations in the analysis. Error bars indicate formal statistical uncertainty derived from random counting. A horizontal dashed line indicates the magnitude for V457 Lac given in the UCAC catalogue (Zacharias *et al.* 2013). The timing of the eclipse is consistent with the ephemeris reported via the AAVSO web site.

Figure 4 shows a light curve for RR Lyr. We observe the star rise from $V \sim 8.1$ to ~ 7.3 before clouds obscured the image around 06:30 UT. The comparison star (UCAC 664-074503) shows no systematic trends (nor does any other star in the field—this star is included as representative). The RMS scatter in the brightness of the comparison star (before the clouds arrived) is ~ 0.01 mag, consistent with the results reported in Figure 3. Since the rise is clearly unique to RR Lyr, greatly exceeds the systematic variability, and coincides with the predicted rise of this target, we are confident that we have robustly detected the variability of this star.

Figure 4 shows a light curve for eclipsing binary V457 Lac. This curve shows a significant dip in the brightness of the system, from an average magnitude of $V \sim 9.8$ to a minimum of ~ 10.0. The comparison star shows no such systematic deviation from a constant brightness. Note that this magnitude range for V457 Lac is in line with the AAVSO reported magnitude range from 9.84 to 10.04. The time of onset for this eclipse is consistent with the 03:00 (UT) time predicted by the ephemeris in the AAVSO Target Tool.

These observations give us confidence in the reliability and accuracy of our tools.

6. Future work

Now that the images from the 16-inch telescope are automatically and reliably reduced and analyzed, we hope to use the facility for scientific studies. Being a small observatory in an urban setting, the most likely venue for us to make meaningful contributions is in the study of bright variables and/or transients. With a typical limiting magnitude of $V \sim 15$ for a 60-s image, many variable stars are within our reach (e.g. Woźniak *et al.* 2004; Paczyński 2006). A few supernovae a year should be visible (e.g. Lae *et al.* 2015; Bellm *et al.* 2019), and occasionally even a Gamma-Ray Burst (e.g. Smith *et al.* 2016) or gravitational wave merger/kilonova event (Abbott *et al.* 2017). Asteroids are also potential targets.

We hope to bring our companion spectroscopic telescope on line soon, and with the two together we hope to monitor spectroscopic binaries for doppler shifts. The ~1% variations at the bright end of our observations means that detecting exoplanet transits will be a challenge. We can improve the statistics with longer exposure times, of course, at the cost of temporal precision in determining the ingress and egress times of the transits.

On the technical side, in addition to the autoguiding capability mentioned previously, we plan to integrate the weather monitoring stations into the operating software so that if the stations detect poor observing conditions, they will automatically trigger a shutdown. Although we have scripting software that can execute a planned set of observations, the observing queue is not dynamical nor does it take elevation into account. We hope to improve this in the future.

Our preliminary analysis of the limiting magnitudes of our images suggests that perhaps our source extraction cutoff of four times the background RMS might be too conservative. For the dimmest stars in the images (around $V \sim 16$), the statistical uncertainty is about 0.03 mag, and the RMS fluctuation over 35 images in one night is only 0.07 mag. This suggests we are not even reaching as far down as a SNR of 10, and we could be missing dimmer stars. For the purposes of the *automated* pipeline, we wanted to err on the conservative side, but we could in the future explore whether that cutoff could be reduced without introducing too many false positives.

In any case, we hope that this report will give future readers confidence in understanding the conditions and limitations under which our observations were taken.

7. Acknowledgements

The authors would like to thank J. Donald Cline for his continuing support of the observatory, as well as colleagues and students at Guilford College for help and discussions. In particular, Prof. T. Espinola, C. Potts, S. Kirwan, N. Cleckler, E. Ruprecht, and A. Jordan have been of great help along the way. K. Iverson, of Plane Wave Instruments, helped with the automation of the dome. K. Sturrock's PYTHON library was critical in enabling us to automate observing in THESKYX, and J. Lynch donated the telescope control computer. Thanks also to Prof. D. Reichart for support in the early phases of this work. We would also like to thank the anonymous referree, whose suggestions were very helpful in improving both this paper and the analysis on which it is based. This research was made possible through the use of the AAVSO Photometric All-Sky Survey (APASS), funded by the Robert Martin Ayers Sciences Fund and NSF AST-1412587.

References

AAVSO. 2017, AAVSO Target Tool (https://www.aavso.org/aavso-target-tool).

Abbott, B. P., *et al.* 2017, *Astrophys. J., Lett.*, **848**, L12.

Akerlof, C. W., *et al.* 2003, *Publ. Astron. Soc. Pacific*, **115**, 132.

Astropy Collaboration, *et al.* 2013, *Astron. Astrophys.*, **558A**, 33.

Aurora Eurotech. 2019, Aurora cloud sensor (http://www.auroraeurotech.com/CloudSensor.php).

Barbary, K. 2016, *J. Open Source Software*, **1**, 58.

Bellm, E. C., *et al.* 2019, *Publ. Astron. Soc. Pacific*, **131**, 078002.

Cinzano, P., Falchi, F., and Elvidge, C. D. 2001, *Mem. Roy. Astron. Soc.*, **328**, 689.

Corbett, M. 2011, Bachelor's thesis, Guilford College.

Davis Instruments. 2019, Vantage Vue weather station (https://www.davisinstruments.com/solution/vantage-vue).

Deep Sky Instruments. 2019, RC optical systems telescope command center (TCC-I; https://www.rcopticalsystems.com/accessories/tcc.html).

Diffraction Limited. 2019a, MAXDOME II observatory dome control system (https://diffractionlimited.com).

Diffraction Limited. 2019b, SBIG STF-8300M CCD camera (https://diffractionlimited.com/product/stf-8300).

Everett, M. E., and Howell, S. B. 2001, *Publ. Astron. Soc. Pacific*, **113**, 1428.

Henden, A. A., Welch, D. L., Terrell, D., and Levine, S. E. 2009, *Bull. Amer. Astron. Soc.*, **41**, 669.

Honeycutt, R. K. 1992, *Publ. Astron. Soc. Pacific*, **104**, 435.

Law, N. M., *et al.* 2015, *Publ. Astron. Soc. Pacific*, **127**, 234.

Ouellette, J. 2016, Bachelor's thesis, Guilford College.

Paczyński, B. 2006, *Publ. Astron. Soc. Pacific*, **118**, 1621.

Seitz, T. 2016, Bachelor's thesis, Guilford College.

Smith, A. B., Caton, D. B., and Hawkins, R. L. 2016, *Publ. Astron. Soc. Pacific*, **128**, 055002.

Smith, D., *et al.* 2003, in *Gamma-Ray Burst and Afterglow Astronomy 2001*, AIP Conf. Proc. 662, American Institute of Physics, Melville, NY, 514.

Software Bisque. 2019a, Paramount ME robotic telescope mount (http://www.bisque.com/sc/media/p/28169.aspx).

Software Bisque. 2019b, THESKYX professional edition (http://www.bisque.com).

Watson, C., Henden, A. A., and Price, C. A. 2006–2014, AAVSO International Variable Star Index VSX (http://www.aavso.org/vsx).

Wells, D. C., Greisen, E. W., and Harten, R. H. 1981, *Astron. Astrophys., Suppl. Ser.*, **44**, 363.

Woźniak, P. R., *et al.* 2004, *Astron. J.*, **127**, 2436.

Zacharias, N., Finch, C. T., Girard, T. M., Henden, A., Bartlett, J. L., Monet, D. G., and Zacharias, M. I. 2013, *Astron. J.*, **145**, 44.